Studies Directed toward Ascertaining the Active Conformation of 1,4-Dihydropyridine Calcium Entry Blockers

George Rovnyak,*† Niels Andersen,# Jack Gougoutas,§ Anders Hedberg,‡ S. David Kimball,† Mary Malley,§ Suzanne Moreland,‡ Michael Porubcan,† and Andrew Pudzianowski§

Departments of Chemistry/Cardiopulmonary, Molecular Modelling/X-Ray Crystallography, and Pharmacology, The Squibb Institute for Medical Research, P.O. Box 4000, Princeton, New Jersey 08543-4000, and Department of Chemistry, University of Washington, Seattle, Washington 98195. *Received August 3, 1987*

A series of unsymmetrically substituted 4-phenyl-1,4-dihydropyridine calcium entry blockers were investigated for their ability to relax potassium-contracted rabbit aortic smooth muscle and to competitively displace [^{3}H]nitrendipine from its specific binding sites on guinea pig myocardial membranes in order to delineate the pharmacologically active conformer with respect to the position of the aromatic substituent (synperiplanar or antiperiplanar). The data show that the 1,4-dihydropyridine receptor distinguishes between 2′,3′-disubstituted phenyldihydropyridines and 2′,5′-disubstituted analogues as measured by changes of vasodilation and receptor affinity in vitro. The IC_{50} values for vasorelaxation by the analogues presented here correlate best with the K_d values for binding to the predominant receptor of two coexisting dihydropyridine binding sites in the guinea pig myocardium. We report the first observation of an antiperiplanar orientation of an *o*-phenyl substituent in the X-ray structure of 2-chlorophenyl analogue **3**. Using nuclear Overhauser enhancement, we have developed a method that also demonstrates that an ortho (chloro or nitro) substituent on the phenyl ring does not preclude the presence of either synperiplanar or antiperiplanar phenyl rotamer in solution. These experimental findings contrast with the accepted belief that *o*-phenyl substituents essentially force these 1,4-dihydropyridines into the synperiplanar conformation exclusively.

Numerous studies underline the positive influence of aromatic substitution on 1,4-dihydropyridine calcium antagonist activity, with the order of potency being ortho > meta ≫ para for both hypotensive[1] and negative inotropic[2] activity. The effect of phenyl substitution on the negative inotropic activity for a series of these compounds has been correlated with the Verloop steric parameter B1[3] for ortho substituents but not with lipophilicity or with electronegativity.[2] The superior efficacy of compounds containing bulky ortho substituents has been attributed to a forced perpendicular orientation between the 4-aryl ring and the 1,4-dihydropyridine ring.[1,2,4] In addition, the crystal structures of a set of 1,4-dihydropyridine calcium entry blockers were determined, and a negative correlation was observed between the magnitude of the 1,4-dihydropyridine ring puckering and relaxation of guinea pig ileal smooth muscle, contracted by the muscarinic receptor agonist *cis*-2-methyl-4-[(dimethylamino)methyl]-1,3-dioxolane methiodide (CD).[5]

In the present investigation, we have focused our attention on determining the pharmacologically active conformer of 3′-substituted phenyl-1,4-dihydropyridine calcium entry blockers and on the conformational preferences exhibited by the 1,4-dihydropyridine receptor, using functional studies of rabbit aorta smooth muscle contraction in vitro and specific radioligand binding in myocardial membranes. An unsymmetrically substituted phenyldihydropyridine may be oriented in either of two minimum-energy conformations, with the substituent on the phenyl ring positioned either toward the C-4 hydrogen (synperiplanar, *sp*) or away from the C-4 hydrogen (antiperiplanar, *ap*) as depicted in figures A and B in Table I. All previously reported solid-state structures for ortho-substituted phenyl-1,4-dihydropyridines show the synperiplanar orientation.[5-10] However, the solid-state conformation need not reflect the conformational preference at the receptor (or in solution).

There is experimental evidence for the rapid rotation of the aromatic ring of a (2′,4′,6′-trimethylphenyl)-1,4-dihydropyridine in solution at room temperature. The authors also reported that the energetically preferred rotamer of the 2′,4′-dimethylphenyl analogue is synperiplanar and concluded that the *o*-methyl group provides a significant bias for the *sp* rotamer in solution.[11] Moreover, a similar conclusion was drawn for an *o*-chlorophenyl-substituted 1,4-dihydropyridine.[12] On the basis of this experimental precedent, we approached the question of aryl ring conformation by synthesizing 4-phenyl-1,4-dihydropyridines with a 2′-chloro substituent in addition to a nitro group at positions 3′, 4′, or 5′ of the phenyl ring on the assumption that the ortho chlorine would strongly bias the conformation of the aromatic ring to a synperiplanar orientation, as suggested in the literature.[11,12] We anticipated that the 2′-chloro, 3′-nitro derivative (**4**) would have the nitro substituent oriented *sp*, while the 2′-chloro, 5′-nitro derivative (**6**) would have the nitro group oriented *ap*, and that receptor preference for these opposing orientations would be reflected in the observed pharmacological potency and receptor affinity. Although we have been able to show a clear enhancement of potency for 2′,3′-disubstituted phenyl-1,4-dihydropyridine (**4**) relative to the corresponding 2′,5′-disubstituted phenyl-1,4-di-

† Department of Chemistry/Cardiopulmonary, The Squibb Institute for Medical Research.
§ Department of Molecular Modelling/X-Ray Crystallography, The Squibb Institute for Medical Research.
‡ Department of Pharmacology, The Squibb Institute for Medical Research.
# Department of Chemistry, University of Washington.

(1) Loev, B.; Goodman, M. M.; Snader, K. M.; Tedeschi, R.; Macko, E. *J. Med. Chem.* **1974**, *17*, 956.
(2) Rodenkirchen, R.; Bayer, R.; Steiner, R.; Bossert, F.; Meyer, H.; Moller, E. *Arch. Pharm. (Weinheim, Ger.)* **1979**, *310*, 69.
(3) Verloop, A.; Hoogenstraaten, W.; Tipker, J. *Drug Design*; Ariens, E. J., Ed.; Academic: New York, 1976; Vol. 7, pp 165–207.
(4) Janis, R. A.; Triggle, D. J. *J. Med. Chem.* **1983**, *26*, 775.
(5) Fossheim, R.; Svarteng, K.; Mostad, A.; Romming, C.; Shefter, E.; Triggle, D. J. *J. Med. Chem.* **1982**, *25*, 126.
(6) Triggle, A. M.; Shefter, E.; Triggle, D. J. *J. Med. Chem.* **1980**, *23*, 1442.
(7) Fossheim, R. *Acta Chem. Scand.* **1985**, *39*, 785.
(8) Fossheim, R. *Acta Chem. Scand.* **1986**, *40*, 776.
(9) Fossheim, R. *J. Med. Chem.* **1986**, *29*, 305.
(10) Fonseca, I.; Martinez-Carrera, S.; Garcia-Blanco, S. *Acta Crystallogr., Sect C: Crystal Struct. Commun.* **1986**, *C42*, 1792.
(11) Goldmann, S.; Geiger, W. *Angew. Chem., Int. Ed. Engl.* **1984**, *23*, 301.
(12) Berntsson, P.; Carter, R. E. *Acta Pharm. Suec.* **1981**, *18*, 221.

0022-2623/88/1831-0936$01.50/0

Table I. Test Compounds, Physical Data, and Rotamer Preferences (Solid State and Solution)

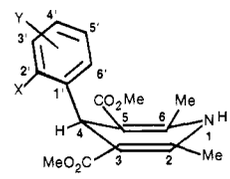

sp-Rotamer
A

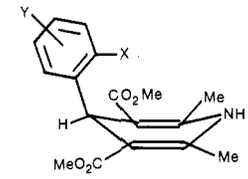

ap-Rotamer
B

						rotamer preference		
							solution:[b]	
no.	X	Y	mp, °C	% yield	R^c	solid state:[a] sp/ap	f_s	K_{eq}
1	H	3′-CN	208–209	25[d]	0.045 ± 0.007	ap[d]	0.41 ± 0.08[e]	0.7 ± 0.2
2	H	3′-NO_2	207–208	60[f]	0.067 ± 0.004	sp[f]	0.52 ± 0.08[e]	1.1 ± 0.3
3	Cl	H	184–186	26[g]	0.16 ± 0.05	sp/ap	0.73 ± 0.09	3 ± 1
4	Cl	3′-NO_2	219–221	16[h]	0.092 ± 0.006	sp	0.60 ± 0.08	1.5 ± 0.5
5	Cl	4′-NO_2	228–229	25[i]	0.22 ± 0.005	sp	0.80 ± 0.05	4 ± 1
6	Cl	5′-NO_2	192–193	21[j]	0.19 ± 0.006	sp	0.77 ± 0.06	3 ± 1
7	H	4′-NO_2	196–197	23[k]				
8	NO_2	H	172–174	27[l]	0.43 ± 0.16	sp[d]	0.90 ± 0.06	9 ± 5

[a] Synperiplanar (*sp*) and antiperiplanar (*ap*) from X-ray crystallographic data. [b] Fraction synperiplanar (f_s) and *sp*/*ap* equilibrium ratio (K_{eq}) as determined by NOE studies (see the Experimental Section for details). [c] NOE ratio and experimental uncertainty limits. [d] Reference 6; no melting point given. [e] Derived with use of the average interproton distances determined for **3**–**6** and **8**, under the reasonable assumption that the distances for **1** and **2** will fall within the same limits. See Molecular Geometries section for details. [f] Literature mp 206–208 °C; ref 42. [g] Reference 2; no melting point given. [h] Recrystallized from ethanol. [i] Recrystallized from methanol. [j] Literature mp 192 °C; ref 44. [k] Literature mp 196–197 °C; ref 44. [l] Nifedipine; lit. mp 172–173 °C; ref 1.

Table II. Vasorelaxant Activity and Receptor Binding Affinity

			NTP binding[a]			
no.	IC_{50},[b] nM	95% CI,[c] nM	$B_{max}1$, %	K_d1, nM	$B_{max}2$, %	K_d2, nM
1	11.1	7.3–16.9	83 ± 3.2	2.15 ± 0.33	17 ± 3.2	152.2 ± 66.5
2	4.0	3.7–4.8	72 ± 3.7	0.13 ± 0.03	28 ± 3.7	29.6 ± 15.3
3	3.0	2.5–3.4	21 ± 12.3	0.006 ± 0.002	79 ± 12.3	1.0 ± 0.12
4	1.0	0.6–1.5	79 ± 1.1	0.23 ± 0.08	21 ± 1.1	85 ± 19.0
5	185	158–234	8 ± 4.8	1.25 ± 1.05	92 ± 4.8	107 ± 13.7
6	13.6	9.8–17.6	49 ± 5.4	0.95 ± 0.25	51 ± 5.4	74.4 ± 25.1
7	3050	2300–4500	100	148 ± 4.4[d]		
8[e]	0.5	0.2–2.0	100	0.39 ± 0.05[d]		

[a] Radioligand–dihydropyridine receptor binding assay. [b] Vasorelaxant assay. [c] 95% fiducial limits for IC_{50}. [d] Monophasic single-site binding analysis. [e] Nifedipine.

hydropyridine (**6**), our studies of the solution conformations of these analogues have demonstrated that there is not an overwhelming bias toward the synperiplanar orientation as implied in the literature. Moreover, we have determined the solid-state structure of 2′-chloro analogue **3** and have found that the aromatic ring is oriented with the chlorine both synperiplanar and antiperiplanar in a ratio of 1:1. This is the first reported case of an antiperiplanar oriented 2′-substituted phenyl-1,4-dihydropyridine in the solid state.

Chemistry

The dihydropyridine analogues **1**–**6** were prepared by using standard methodology[13] and commercially or synthetically available benzaldehyde derivatives. Pertinent physical, analytical, and spectral data for new compounds are given in the Experimental Section.

Pharmacology

Circumferential strips of rabbit thoracic aorta were contracted by depolarization with high extracellular concentrations of potassium and then relaxed by exposure to various concentrations of the dihydropyridines. IC_{50} values (the concentration of compound that caused 50% relaxation) were calculated and are shown in Table II. This test has been shown to be relatively diagnostic for calcium entry blockade.[15] Dihydropyridine receptor affinity was determined by inhibition of [^{3}H]nitrendipine binding to guinea pig myocardial membranes. It is generally accepted that dihydropyridine radioligand–receptor binding in cardiac tissue represents a system whereby a functionally relevant interaction of putative ligands may be studied.[16-18] Details of these assay methods and analyses are provided in the Experimental Section.

Results and Discussion

Structure–Biological Activity Studies. Depolarization of vascular smooth muscle with high extracellular concentrations of potassium has been shown to be associated with the influx of calcium through voltage-dependent slow calcium channels in the sarcolemma.[19,20] As

(13) Bossert, F.; Meyer, H.; Wehinger, E. *Angew. Chem., Int. Ed. Engl.* **1981**, *20*, 762.
(14) Brittain, R. J.; Moreland, S. *Physiologist* **1985**, *28*, 325.
(15) Ehlert, F. J.; Etoza, E.; Rocske, W. R. *Biochem. Biophys. Res. Commun.* **1982**, *104*, 931.
(16) Belleman, P.; Ferry, D.; Glossman, H. *Arzneim.-Forsch.* **1981**, *31*, 2064.
(17) Depover, A.; Lee, S. W.; Matlib, M. A.; Whitmer, K.; Davis, B. A.; Powell, T.; Schwartz, A. *Biochem. Biophys. Res. Commun.* **1983**, *113*, 185.
(18) vanBreeman, C.; Fannas, B. R.; Gerba, P.; McNaughton, E. D. *Circ. Res.* **1972**, *30*, 44.
(19) Mras, S.; Sperelakis, N. *Eur. J. Pharmacol.* **1981**, *71*, 13.

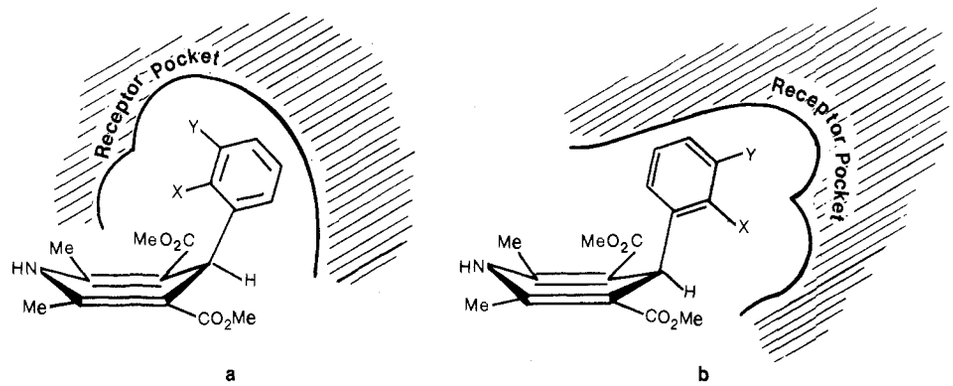

Figure 1. These schematics show the putative orientation of the test compounds at the dihydropyridine receptor. The potential shape of the lipophilic pocket is depicted when the receptor pocket is occupied by the antiperiplanar aryl rotamer (a) or the synperiplanar aryl rotamer (b).

the intracellular concentration of calcium increases, the smooth muscle cells contract. These contractions can be either prevented or reversed by exposing the cells to dihydropyridine calcium entry blockers.[21,22] Based on results from this method of evaluating calcium entry blockade, our data (Table II) suggest a difference between the 3′- and 5′-aryl positions with respect to both smooth muscle relaxant activity and receptor binding affinity. Thus, the 2′-chloro-3′-nitrophenyl analogue **4** is the most potent vasorelaxant in the series, with the exception of nifedipine **8**, which is included as a reference compound. The activity of the 2′-chloro, 5′-nitrophenyl analogue **6** was 14 times less than that of **4**, providing evidence for the nonequivalency of the 3′- and 5′-phenyl positions in these compounds with respect to their potency as calcium entry blockers (as determined in the potassium-contracted rabbit aorta assay). The 2′-chloro-4′-nitrophenyl analogue **5** was found to be much less active than either **4** or **6**, a result that is consistent with the well-known detrimental effect of 4-phenyl substitution in this class of calcium entry blockers.[1,2] These data demonstrate a clear enhancement of potency for 2′,3′-disubstituted phenyl-1,4-dihydropyridines (**4**) relative to the corresponding 2′,5′-disubstituted phenyl-1,4-dihydropyridines (**6**). We can, therefore, ascribe this same preference to the 1,4-dihydropyridine receptor, wherein the positive steric interaction at the 2′-phenyl position may extend to include a favorable interaction with a nitro substituent at the adjacent 3′-position but may not encompass a substituent at the 5′-position. These two preferences are illustrated schematically in Figure 1a,b for the *ap* and *sp* conformations, respectively, of an unsymmetrically substituted 1,4-dihydropyridine at the dihydropyridine receptor.

For comparative purposes, we included the monosubstituted 3′-cyano (**1**) and 3′-nitro (**2**) analogues in this study as these compounds have been reported[5,6] to possess opposite orientations of the phenyl substituent in the solid state (**1**, *ap* and **2**, *sp*). We did not observe a large difference between the vasorelaxant properties of **1** and **2** for inhibition of potassium-contracted rabbit aorta smooth muscle, which is consistent with the results reported by Triggle and co-workers for the ability of **1** and **2** to relax either potassium-contracted or muscarinic agonist (CD) contracted guinea pig ileum.[23]

The compounds of this study were also examined for their ability to compete with [^{3}H]nitrendipine for the 1,4-dihydropyridine receptors on guinea pig myocardial membranes. The specific binding of [^{3}H]nitrendipine was characterized with regard to kinetics, saturability, and competitive inhibition. Kinetic analysis of the specific binding of nitrendipine revealed a dissociation constant (K_d) of 0.13 ± 0.05 nM ($k_1 = 3.03 \times 10^8$ M^{-1} min^{-1}; k_{-1} = 0.04 M^{-1} min^{-1}; $n = 6$). Analysis of the saturation binding isotherm yielded a K_d value of 0.48 ± 0.03 nM and a density of specific binding sites of 220.3 ± 10.4 fmol/mg of protein ($n = 18$).

The unlabeled test compounds were found to completely inhibit the specific binding of [^{3}H]nitrendipine to guinea pig myocardial membranes. With the exceptions of compounds **5**, **7**, and **8**, all concentration–inhibition curves were characterized by slope factors of less than 0.75 when analyzed for radioligand interaction on a single hypothetical class of binding sites. Binding data were routinely analyzed by using a hypothetical two-site receptor model for the curves that had slopes of less than 0.9 when analyzed by a single-site binding equation. This procedure yielded a statistically significant improvement in fitting the computer-generated curves to the data points of compounds **1**–**6** as compared to fitting the data points to a single-site curve. Compounds **1**, **2**, and **4** were found to display a biphasic inhibition of radioligand binding with high affinity for an apparently predominant class of binding sites, whereas compounds **3**, **5**, and **6** bound to a high-density class of binding sites with relatively low affinity. Compound **7** was found to bind to a single recognition site with comparatively low affinity. Nifedipine (**8**), on the other hand, was found to bind to a single recognition site with relatively high affinity (Table II).

An attempt was made to find a correlation between functional inhibitory values (IC_{50} values from rabbit aorta assay) and receptor affinity values (K_d values from radioligand binding in myocardium). The IC_{50} values were plotted against either the corresponding high affinity values (Figure 2a), the corresponding low affinity values (Figure 2b) or the corresponding affinity value derived from binding to the predominant class of receptors determined from analysis of biphasic inhibition curves (Figure 2c). The correlation coefficients were 0.70, 0.59, and 0.85 with linear slopes of 0.81, 0.49, and 0.86, respectively. These data suggest that the functional calcium entry blocking potency is best correlated with binding of the compounds to a single high-density receptor component. The observed correlation between functional calcium entry blocking potency in depolarized smooth muscle and affinity for a predominant cardiac receptor population may

(20) Sperelakis, N.; Mras, S. *Blood Vessels* **1983**, *20*, 172.
(21) Mras, S. *J. Cardiovasc. Pharmacol.* **1986**, *8* (Suppl. 8), S80.
(22) Bolger, G. T.; Gengo, P.; Klockowski, R.; Luchowski, E.; Siegel, H.; Janis, R. A.; Triggle, A. M.; Triggle, D. J. *J. Pharm. Exp. Ther.* **1983**, *225*, 291.
(23) Miyamae, A.; Koda, S.; Morimoto, Y. *Chem. Pharm. Bull.* **1986**, *34*, 3071.

Table III. Crystal Data

	3 (PrOH)[a]	4 (EtOH)	5 (MeOH)	6 (MeCN)
a, Å	13.467 (2)	31.799 (4)	11.233 (1)	15.658 (6)
b, Å	13.718 (2)	11.561 (1)	17.663 (1)	12.686 (5)
c, Å	9.867 (1)	9.470 (1)	8.885 (1)	8.936 (3)
α, deg	98.44 (1)	90.	90.	90.
β, deg	93.25 (1)	90.	90.	90.
γ, deg	65.40 (1)	90.	90.	90.
V, Å^3	1639.4 (6)	3481.6 (8)	1762.9 (4)	1775. (2)
space group	$P\bar{1}$	$Pbca$	$P2_12_12_1$	$Pnma$
D_{obsd}, g cm^{-3}	1.35	1.44	1.43	1.42
D_{calcd}, g cm^{-3}	1.36	1.453	1.435	1.43
Z	4	8	4	4
max 2θ, deg	140	140	140	140
NREF[b]	4226	2459	1552	1774
NOBS[c]	2765	1502	1322	1195
NVAR[d]	416	236	236	137
R	0.055	0.061	0.036	0.057
R_w	0.065	0.074	0.046	0.063

[a] Solvent of recrystallization. [b] Total number of symmetry independent measured reflections. [c] Total number of "observed" reflections with $I \geq 3\sigma(I)$ used for refinement. [d] Number of variables in least-squares refinements.

indicate that the 1,4-dihydropyridine receptors in the rabbit aorta have properties similar to those of a predominant class of receptors in the guinea pig myocardium. It is possible that the biphasic binding characteristics are not necessarily relevant for the pharmacological action of the compounds and that the nonideal kinetics are due to restricted access to various fractions of the receptor pool under the present experimental conditions. In this case, the high-density class of receptors may simply represent the bulk fraction of uniformly accessible receptors localized to the extracellular surface of the plasma membrane.

Compounds **3–6** and **8** lowered blood pressure in spontaneously hypertensive rats following oral administration (data not shown). The order of potency was similar to that observed by examination of the IC_{50} and K_d values. These data suggest that receptor binding, vascular smooth muscle relaxation, and antihypertensive activity may all be expressions of a single mechanism of action for these compounds.

Solid State and Solution Conformational Studies. Goldmann and Geiger have concluded for a 2′,4′-dimethylphenyl-1,4-dihydropyridine analogue[11] that the ortho substituent heavily biases the phenyl ring toward the synperiplanar orientation (figure A, Table I) in solution. Berntsson and Carter have drawn a similar conclusion for 2′-chlorophenyl analogues.[12] Both studies relied on evidence that demonstrated the presence of the synperiplanar orientation but only inferred the relative absence of the antiperiplanar orientation.

In contrast, our approach to determining rotamer populations in solution is based upon a direct measurement of both synperiplanar (NOE of NH to ortho aryl H) and antiperiplanar (NOE of methine CH to ortho aryl H) conformations. Normalized transient ΔNOE spectra permitted the calculation of phenyl rotamer populations using interatomic distances derived from experimentally determined crystallographic and AM1 energy minimized structures (Tables III–VI). Details of this method are

Table IV. Experimental and Calculated Geometric Parameters of Test Compounds

no.	X	Y	conformer	source[b]	rms,[c] Å	d_N,[d] Å	d_C,[e] Å	θ, deg
3[a]	Cl	H	*sp*	crys	0.001	0.131	0.342	14.4
				AM1	0.002	0.202	0.270	19.6
			ap	crys	0.002	0.102	0.212	29.3
				AM1	0.002	0.068	0.200	28.1
4	Cl	3′-NO_2	*sp*	crys	0.008	0.062	0.135	26.7
				AM1	0.001	0.153	0.225	22.2
			ap	AM1	0.001	0.068	0.171	30.0
5	Cl	4′-NO_2	*sp*	crys	0.006	0.109	0.202	24.2
				AM1	0.000	0.205	0.270	19.2
			ap	AM1	0.000	0.058	0.169	29.5
6	Cl	5′-NO_2	*sp*	crys	0.000	0.174	0.330	16.9
				AM1	0.001	0.194	0.284	18.2
			ap	AM1	0.001	0.067	0.165	29.9
8	NO_2	H	*sp*	crys	0.019	0.090	0.251	20.3
				AM1	0.003	0.120	0.181	25.2
			ap	AM1	0.005	0.073	0.228	25.8

[a] Compound number (see Table I). [b] "crys" refers to crystal structures. [c] Root-mean-square deviation of atoms 2, 3, 5, and 6 from their least-squares plane. [d] Perpendicular displacement of N1 from the least-squares plane in the direction of the phenyl ring. [e] Perpendicular displacement of C4 from the least-squares plane in the direction of the phenyl ring.

Table V. Experimental and Calculated Interproton Distances and Calculated Enthalpies of Formation

no.	X	Y	conformer	source	H1–H6′, Å	H4–H6′	$\Delta H_f°$ (AM1),[a] kcal/mol
3	Cl	H	*sp*	crys	3.189	3.786	
				AM1	3.422	3.795	−123.7
			ap	crys	6.478	2.212	
				AM1	6.487	2.148	−123.0
4	Cl	3′-NO_2	*sp*	crys	3.583	3.750	
				AM1	3.498	3.782	−115.6
			ap	AM1	6.500	2.137	−116.2
5	Cl	4′-NO_2	*sp*	crys	3.565	3.757	
				AM1	3.348	3.797	−120.4
			ap	AM1	6.507	2.152	−120.9
6	Cl	5′-NO_2	*sp*	crys	3.232	3.793	
				AM1	3.268	3.797	−121.2
			ap	AM1	6.512	2.150	−121.4
8	NO_2	H	*sp*	crys	3.419	3.729	
				AM1	3.624	3.728	−111.1
			ap	AM1	6.397	2.170	−112.1

[a] Calculated enthalpies of formation of AM1 optimized geometries of test compounds.

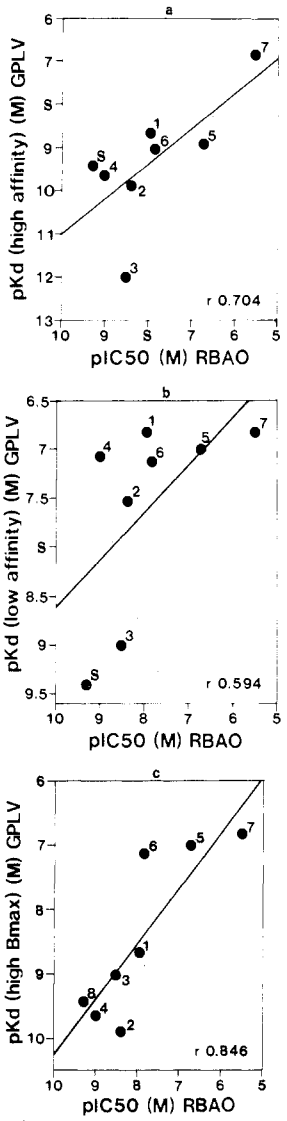

Figure 2. Graphs showing the correlation between the IC_{50} for relaxation of K^+-contracted rabbit aorta and the K_d for NTP binding in guinea pig myocardial membranes. The K_d values plotted were obtained from binding to the high-affinity sites (a), the low-affinity sites (b), or the predominant sites (c) as determined from analysis of biphasic inhibition curves. The correlation coefficients were 0.70 (a), 0.59 (b), and 0.85 (c), indicating that the functional calcium entry blockade observed in the vasorelaxant assay may be the result of binding to a single high-density receptor component.

Table VI. Average Interproton Distances Used in Eq 3 To Derive Fraction of Synperiplanar Conformer

	average geometries
sp	
θ	20.5 ± 4.6°
s_1	3.40 ± 0.16 Å
s_4	3.76 ± 0.02 Å
ap	
θ	28.7 ± 4.6°
a_1	6.48 ± 0.16 Å
a_4	2.15 ± 0.02 Å

described in the Experimental Section. The question of conformer preference in solution may be addressed directly by considering the equilibrium $ap \rightleftharpoons sp$. The equilibrium constant (K_{eq}) for this process is simply the conformer ratio, which may be determined from the equation:

$$K_{eq} = \frac{[sp]}{[ap]} = \frac{f_s}{1 - f_s} \quad (1)$$

where f_s is the fraction synperiplanar conformation obtained from the NOE results. The values obtained for the compounds studied here are reported in Table I, along with uncertainty limits derived from a differential error analysis of eq 1.

For meta-substituted analogues 1 and 2, both rotamers were observed in essentially equal amount, a result consistent with the literature[23] for another meta-substituted phenyl analogue. Unexpectedly, our analysis of the solution conformations of the 2′-chloro analogues 3–6 shows only a small energetic bias for the synperiplanar rotamer, a result that appears to contrast with the previous literature[11,12] in this area. Also, our data show that nifedipine (8), a 2′-nitrophenyl analogue, exhibits a similar, nonexclusive preference for the synperiplanar rotamer in solution. (It is interesting to note that only 1 has an equilibrium constant favoring the antiperiplanar conformer, and that only 1 has been observed[6] to crystallize exclusively in the *ap* conformation.) The Gibbs free energy differences corresponding to these equilibrium constants are quite small at room temperature. Therefore, we can conclude for the ortho-substituted phenyl compounds presented here that the antiperiplanar rotamer cannot be excluded from consideration as the active rotamer at the receptor.

The solid-state structures of many 1,4-dihydropyridines have been described. Without exception, all analogues having a substituent in the ortho position of the phenyl ring are reported to crystallize in the synperiplanar orientation.[5-10] We report the first example (2′-chloro analogue 3) of an ortho-substituted phenyl-1,4-dihydropyridine that crystallizes in the antiperiplanar orientation. Actually, two independent molecules are present in the crystal structure of 3. One adopts the synperiplanar orientation and the other adopts the antiperiplanar orientation (Figure 3a,b). This observation lends further support to the NMR results, demonstrating that an ortho substituent on the phenyl ring does not provide significant energetic bias toward the synperiplanar rotamer. AM1 calculations (for ortho-substituted analogues 3–6 and 8) also support this view. The calculated enthalpies of formation for each *sp*/*ap* pair of conformers are not significantly different (Table V), suggesting that little intrinsic energetic preference exists for either conformer.

Several other groups have examined the importance of phenyl orientation and substituent position for the active conformation of 1,4-dihydropyridines. In one approach, compounds containing lactone bridges of increasing size between the phenyl and carboxyl groups were prepared.[24-26] For these compounds, both receptor binding affinity (K_i, [^{3}H]nimodipine displacement) and in vitro potency (relaxation of potassium-contracted rabbit aortic rings) increased as the phenyl ring approached an orientation perpendicular to the dihydropyridine ring. Using another approach, Hartman and co-workers[27,28] and

(24) Seidel, W.; Meyer, H.; Born, L.; Kazda, S.; Dompert, W. *Abstracts of Papers*, 187th National Meeting of the American Chemical Society, St. Louis, MO; American Chemical Society: Washington, DC, 1984.
(25) Seidel, W.; Meyer, H.; Born, L.; Kazda, S.; Dompert, W. *Proc. Eur. Symp. Quant. Struct.-Act. Relat., 5th* [*54QWAZ*] 1984, 366–9.
(26) Seidel, W.; Kazda, S.; Knorr, A. Ger. Offen. DE 3235221 A1, 1984.
(27) Hartman, G. D.; Halczenko, W.; Phillips, B. T. *Abstracts of Papers*, 189th National Meeting of the American Chemical Society, Miami, FL; American Chemical Society: Washington, DC, 1985.
(28) Hartman, G. D.; Halczenko, W.; Phillips, B. T. *J. Org. Chem.* 1986, *51*, 142.

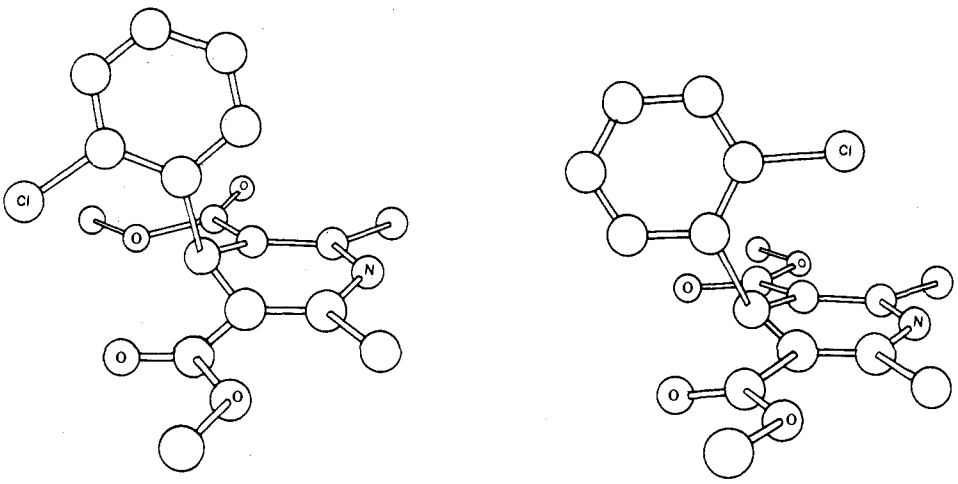

Figure 3. The solid-state structure of 2′-chloro analogue **3**, showing synperiplanar (a) and antiperiplanar (b) orientations of the 2′-chlorophenyl ring.

Claremon and co-workers[29,30] prepared compounds in which the phenyl ring was bridged to the carbon adjacent to the dihydropyridine nitrogen atom. The pharmacological results for compounds having a bridge between the phenyl and dihydropyridine rings suggest a preference at the receptor for the 3′-phenyl substituent in the synperiplanar position for these rigid analogues.[30]

From our studies on nonrigid dihydropyridines, we can conclude for ortho-substituted 4-phenyl-1,4-dihydropyridine calcium entry blockers that an additional substituent is preferred pharmacologically at the 3′-position of the aromatic ring, relative to the 5′-position. However, the results of our NOE experiments preclude defining whether the conformation of these ortho-substituted phenyl analogues at the 1,4-dihydropyridine receptor is synperiplanar or antiperiplanar, because we have shown that both exist in solution, with no overwhelming bias for either conformer.

Summary

In summary, we have examined a simple set of 1,4-dihydropyridines for their ability to relax potassium-contracted rabbit aorta smooth muscle (IC_{50}) and to displace [^{3}H]nitrendipine from its receptor (K_d) in order to delineate the active conformer with respect to unsymmetrically substituted 4-phenyl analogues. The rabbit aorta IC_{50} values correlate best with the K_d for binding to the predominant receptor of two coexisting binding sites in the guinea pig myocardium, suggesting a relationship between receptor occupancy and functional effect.[22] Our data show that the dihydropyridine receptor distinguishes between 2′,3′-disubstituted phenyldihydropyridines and 2′,5′-disubstituted analogues in terms of both function and receptor affinity. In contrast to what has been reported in the literature,[11,12] the direct measurement of phenyl rotamer populations in solution using nuclear Overhauser enhancement shows that these 1,4-dihydropyridines are characterized by a sizeable fraction of both *sp* and *ap* phenyl rotamers. Also, we report the first example of an antiperiplanar oriented ortho-substituted phenyl-1,4-dihydropyridine in the solid state, further suggesting the energetic accessibility of either rotamer of such compounds at the receptor. It is, therefore, impossible to determine from this approach whether the preferred conformation of nonrigid analogues at the dihydropyridine receptor is synperiplanar or antiperiplanar. Examination of this question, along with other details of binding at the 1,4-dihydropyridine receptor, is continuing and will be the subject of future communications.

Experimental Section

Chemistry. Melting points were taken on a Thomas-Hoover capillary melting point apparatus and are uncorrected. Infrared spectra were recorded with a Perkin-Elmer 983 spectrometer in KBr pellets or with a Perkin-Elmer 137 spectrometer as a Nujol mull. ^{1}H NMR spectra were recorded on a JEOL GX-400 or FX-270 spectrometer and were referenced to internal TMS. Microanalyses of all compounds were within ±0.4% of the calculated values.

4-(2-Chloro-3-nitrophenyl)-1,4-dihydro-2,6-dimethyl-3,5-pyridinedicarboxylic Acid, Dimethyl Ester (4). A solution of 2-chloro-3-nitrobenoic acid (2.01 g, 0.01 mol) and ethyl chloroformate (1.08 g, 0.01 mol) in dry THF (25 mL) under argon at room temprature was treated with triethylamine (1.01 g, 0.01 mol) in THF (10 mL) over a 15-min period. After 1 h the solids were removed by filtration, and the filtrate was treated dropwise with $NaBH_4$ (0.5 g, 0.013 mol) in 3 mL of water. After the mixture was stirred overnight, the solvent was removed in vacuo and the residue, dissolved in EtOAc, was washed with H_2O, dilute $NaHCO_3$, water, 1 N HCl, H_2O, and saturated brine. The dried (anhydrous Mg_2SO_4) solution was concentrated in vacuo to give 1.69 g of a crude solid. Hexane trituration afforded 1.5 g (80%) of 2-chloro-3-nitrobenzyl alcohol: mp 67–70 °C; ^{1}H NMR ($CDCl_3$) δ 4.87 (s, CH_2); IR (Nujol) 3250 cm^{-1} (broad, CH_2OH). Anal. ($C_7H_6ClNO_3$) C, H, N, Cl.

2-Chloro-3-nitrobenzyl alcohol (1.87 g, 0.01 mol) was oxidized by the method of Swern[31] to give 1.5 g (79% recrystallized yield from hexane) of 2-chloro-3-nitrobenzaldehyde: mp 93–95 °C (lit.[32] mp 95–96 °C); ^{1}H NMR ($CHCl_3$) δ 10.5 (s, CHO); IR (Nujol) 1700 cm^{-1} (CH=O). Anal. ($C_7H_4ClNO_3$) C, H, N, Cl.

A mixture of 2-chloro-3-nitrobenzaldehyde (1.26 g, 6.35 mmol) and methyl acetoacetate (1.5 g, 12.7 mmol) in 6 mL of EtOH containing 1 mL of concentrated NH_4OH was heated at reflux temperature for 18 h. The cooled reaction mixture, dissolved in EtOAc, was washed with H_2O and saturated brine, dried (anhydrous $MgSO_4$) and concentrated in vacuo. The residue was purified by flash chromatography (CH_2Cl_2/EtOAc, 30:1) to give 0.6 g of amorphous powder. Crystallization from MeOH gave 0.39 g (16%) of **4**: mp 219–221 °C; ^{1}H NMR ($CDCl_3$) δ 2.33 (s, 6 H,

(29) Claremon, D. A.; Hirshfield, J.; Lumma, P. K.; McClure, D. E.; Springer, J. P. *Syntheses* **1986**, 144.
(30) Baldwin, J. J.; Claremon, D. A.; Lumma, P. K.; McClure, D. E.; Rosenthal, S. A.; Winquist, R. J.; Faison, E. P.; Kaczorowski, G. J.; Trumble, M. J.; Smith, G. M. *J. Med. Chem.* **1987**, *30*, 690.
(31) Omura, K.; Swern, D. *Tetrehedron* **1978**, *34*, 1651.
(32) Ricci, A.; Martani, A.; Graziani, O.; Oliva, L. M. *Ann. Chim.* **1963**, *53*, 1860; *Chem. Abstr.* **1964**, *60*, 12000*g*.

CH_3), 3.62 (s, 6 H, OCH_3), 5.53 (s, 1 H, NH), 7.27 (dd, J = 8 Hz, 1 H, aryl), 7.47 (dd, J = 1, 8 Hz, 1 H, aryl), 7.62 (dd, J = 1, 8 Hz, 1 H, aryl); IR (KBr) 1709 cm^{-1} (CO_2Me). Anal. ($C_{17}H_{17}N_2ClO_6$) C, H, N, Cl.

4-(2-Chloro-4-nitrophenyl)-1,4-dihydro-2,6-dimethyl-3,5-pyridinedicarboxylic Acid, Dimethyl Ester (5). A mixture of 2-chloro-4-nitrobenzaldehyde (3.0 g, 16.2 mmol) and methyl acetoacetate (3.5 g, 33.0 mmol) in 8 mL of MeOH containing 4 mL of concentrated NH_4OH was heated at reflux temperature for 18 h. The reaction mixture was diluted with MeOH and allowed to crystallize to give 1.43 g (25%) of **5**: mp 228–229 °C; ^1H NMR ($CDCl_3$) δ 2.30 (s, 6 H, CH_3), 3.65 (s, 6 H, OCH_3), 5.48 (s, 1 H, CH), 6.03 (s, 1 H, NH), 7.56 (d, J = 8 Hz, 1 H, aryl), 7.98 (dd, J = 2, 8 Hz, 1 H, aryl), 8.12 (d, J = 2 Hz, 1 H, aryl); IR (KBr) 1703 cm^{-1} (CO_2Me). Anal. ($C_{17}H_{17}N_2ClO_6$) C, H, N, Cl.

X-ray Determination. Crystal data and some details of the structure refinements are given in Table III. The unit cell parameters were obtained through a least-squares analysis of the experimental diffractometer settings of 15 high angle reflections. Crystal densities were measured by flotation in carbon tetrachloride/hexane mixtures. Intensities were measured on a SYNTEX P21 diffractometer using Cu Kα radiation (λ = 1.5418 Å) at 23 °C with the θ–2θ variable scan technique and were corrected only for Lorentz–polarization factors. Background counts were collected at the extremes of the scan for half of the time of the scan. Two standard reflections were measured every 50 reflections with no decrease of intensity during the course of the measurements.

Structures were solved by direct methods[33] and refined on the basis of "observed" reflections with $I \geq 3\sigma$. All calculations utilized the SDP program[34] package with minor local modifications. The least-squares weights $w = \sigma^{-2}(F_o)$ were calculated with the assumption that $\sigma^{-2}(I) = \epsilon^2 + (pI)^2$ where ϵ is the statistical counting error and p = 0.02–0.04. The function minimized in the least-squares refinement is $\sum_w(|F_o| - |F_c|)^2$. R is defined as $\sum||F_o| - |F_c||/\sum|F_o|$ while R_w is defined as $[\sum_w(|F_o| - |F_c|)^2/\sum_w(F_o)^2]^{1/2}$. Most hydrogen positions were observed on difference maps during the latter stages of refinement. The N1 proton was introduced in its observed position while all other protons were introduced in idealized positions. The scattering of all the hydrogens was taken into account in the terminal stages of refinement. Final difference maps contained no significant features. Tables of atomic coordinates, thermal parameters, bond distances, and bond angles are included as supplemental material.

Nuclear Magnetic Resonance Procedure. Proton NMR spectra were obtained at 400 MHz on a JEOL GX-400 NMR spectrometer equipped with a 5-mm proton probe. Spectral conditions were 32K time domain data points, 6000-Hz spectral width, 4-μs acquisition pulse (90° pulse: 10.5 μs), 4.7-s repetition rate, and 0.2-Hz line-broadening factor. A typical spectrum required 40–120 pulses to achieve the desired signal-to-noise ratio. All spectra were run at 30 °C and were referenced to internal TMS.

Transient (selective inversion) difference NOE spectra[35] were collected directly in memory using the pulse sequence:

$$\Delta\text{NOE} = \{[\text{RD} - {}^{s}\theta^{on} - \tau - {}^{ns}\theta - \text{Acq}(t_2)]_8 - [\text{RD} - {}^{s}\theta^{off} - \tau - {}^{ns}\theta - \text{Acq}(t_2)]_8\}_n$$

A typical experiment used a relaxation delay (RD) of 4 s, an NOE buildup time (τ) of 650 ms, and an acquisition time (t_2) of 2.7 s. The nonselective pulse ($^{ns}\theta$) was usually set to 45°. The selective pulse ($^{s}\theta$) corresponded to a 40-ms decoupler pulse at a power setting of 8.3 Hz ($\gamma B_2/2\pi$). At this power level a 60 ± 5 ms pulse was required to produce a selective 180° flip of a resonance. A typical difference FID required a value of $n \geq 10$.

The NOE ratios (R) in Table I were calculated from the ratio of observed NOE intensities for the ortho proton of the aromatic ring upon irradiation of the NH and CH protons, respectively. To facilitate integrations, all spectra were base line corrected in the region of interest. Difference FID spectra to be compared were subjected to an automatic normalized transform and careful integrations were recorded for the aromatic region as well as for the irradiated peak. For each compound studied, the observed NOE intensities were corrected for variation in irradiation efficiencies and decay rate by residual driver normalization.[36] This correction was calculated from the difference in the area measured for the residual inverted CH and NH peaks in the difference spectra. In some cases, an additional correction for the nonselectivity of the irradiating pulse ($^{s}\theta$) was calculated from the fractional perturbation (area) of the CH or NH peak measured when the other peak was inverted. The NOE ratios for the 3′-substituted compounds **1** and **2** were calculated from the sum of the areas for both ortho protons.

Molecular Geometries, Calculations, and Error Analysis. In this study, the fraction of synperiplanar conformer (f_s) for a specified compound is related to the NOE ratio R by eq 2, where

$$R = \frac{\text{NOE(H1–H6′)}}{\text{NOE(H4–H6′)}} = \frac{(f_s/s_1^6) + [(1 - f_s)/a_1^6]}{(f_s/s_4^6) + [(1 - f_s)/a_4^6]} \quad (2)$$

s_1 is the H1–H6′ distance in the sp conformation, s_4 is the H4–H6′ distance in the sp conformation, a_1 is the H1–H6′ distance in the ap conformation, and a_4 is the H4–H6′ distance in the ap conformation. Rewritten in appropriate form, the fraction of synperiplanar conformer (f_s) can be calculated from eq 3. The

$$f_s = (a_4^6 - Ra_1^6)\left[Ra_1^6\left(\frac{a_4^6}{s_4^6} - 1\right) + a_4^6\left(1 - \frac{a_1^6}{s_1^6}\right)\right]^{-1} \quad (3)$$

inclusion of the s_4 term is essential since this distance is only slightly greater than a_4, and the s_4 term could be significant in the observed NOE for H6′ upon irradiation of H4 when the sp conformer predominates. A standard differential error propagation analysis[37] was applied to eq 3 to derive uncertainty limits for the calculated results.

The determination of suitable distances, and their corresponding uncertainty limits, for use in eq 3 required the use of data from crystal structures and geometry optimizations. The crystallographic analyses did not give hydrogen positions and only one ortho-substituted phenyl-1,4-dihydropyridine crystal structure (**3**) was currently available for an ap conformer. We investigated the use of geometry optimization with the recently developed AM1 semiempirical quantum chemical method;[38,39] this method is expected to be more reliable[38] than the MNDO method from which it was derived, but it was previously untested in this series of compounds.

Total geometry optimizations (all geometric variables allowed to relax) were started from crystal structures where these were available, with hydrogens introduced at approximate positions. Otherwise, optimizations were begun from AM1 structures with appropriate modifications to the phenyl substituents and ester orientations. In all cases, geometry optimization was continued until the energy-gradient components were less than 1.0 kcal mol^{-1} $Å^{-1}$ in absolute magnitude, although most of the final values were actually less than 0.5 kcal mol^{-1} $Å^{-1}$.

To systematize the analysis of molecular geometries, we introduced a least-squares plane fitted to the sp^2 carbons of the DHP ring, i.e., those at positions 2, 3, 5, and 6. A measure of the DHP ring pucker was then afforded by the perpendicular displacements of N1 and C4 from this plane. The angular separation between the DHP and phenyl rings was gauged by the angle θ between

(33) Main, P.; Hull, S. E.; Lessinger, L.; Germain, G.; DeClercq, J.-P.; Woolfson, M. M. *MULTAN 80*, University of York, England and Louvain, Belgium.
(34) SDP, Structure Determination Package, A. Frenz & Associates, College Station, TX 77840.
(35) Andersen, N. H.; Nguyen, K. T.; Eaton, H. L. *J. Magn. Reson.* **1985**, *63*, 365.
(36) Andersen, N. H.; Nguyen, K. T.; Hartzell, C. J.; Eaton, H. L. *J. Magn. Reson.* **1987**, *74*, 195. Eaton, H. L.; Andersen, N. H. *Ibid.* **1987**, *74*, 212.
(37) Shoemaker, D. P.; Garland, C. W. *Experiments in Physical Chemistry*, 2nd ed.; McGraw-Hill: New York, 1967; pp 17–37.
(38) Dewar, M. J. S.; Zoebisch, E. G.; Healy, E. F.; Stewart, J. J. P. *J. Am. Chem. Soc.* **1985**, *107*, 3902.
(39) Dewar Research Group; Stewart, J. J. P. *QCPE* **1986**, *6*, 506. This AMPAC program has been given several minor modifications. All calculations were carried out on VAX 11/750 and 11/785 computers at The Squibb Institute for Medical Research.

the C4–C1′ bond and a vector normal to the least-squares plane. These measurements are reported in Table IV.

To obtain the H–H distances for use in eq 3, we added hydrogens to the available crystal structures at positions consistent with the corresponding AM1 optimized geometries. The resulting distances, as well as those derived from the AM1 optimized geometries, are reported in Table V.

Considerable conformational flexibility is evidenced by the variation in θ and the derived H1–H6′ distances in the experimental solid-state structures of the *sp* conformers (Tables IV and V). The distance H4–H6′, on the other hand, is intrinsic to the benzylic moiety and remains constant within approximately ±0.02 Å. The much smaller variability of the AM1 geometries, which represent molecules in the gas phase, suggests that the crystal structures reflect the influence of solid-state forces on an inherently flexible average geometry. This is supported by additional AM1 calculations which indicate that displacements of ±5° in θ in a given optimized geometry correspond to enthalpy differences of less than a few tenths kcal/mol.

Following this analysis, the crystal structures for the *sp* conformers were treated as multiple experimental observations of an average "intrinsic" structure; accordingly, the corresponding results in Tables IV and V were averaged (see Table VI) to obtain $\theta = 20.5 \pm 4.6°$ (compared with $20.9 \pm 2.6°$ for the AM1 geometries) and the H–H distances $s_1 = 3.40 \pm 0.16$ Å and $s_4 = 3.76 \pm 0.02$ Å (compared with AM1 values of $s_1 = 3.43 \pm 0.06$ and $s_4 = 3.78 \pm 0.01$ Å, respectively). The uncertainties reported with these values represent two standard errors for the arithmetic mean.[37]

For the *ap* conformers, H–H distances had to be derived almost entirely from AM1 geometries. (From the results just described for the *sp* conformers, it is reasonable to expect that average geometrical parameters derived from AM1 will be reliable.) The H1–H6′ distances (a_1) in eq 3 are so large that they contribute little to the calculated fraction synperiplanar (f_s). Furthermore, the H4–H6′ distance (a_4) in eq 3 is intrinsic to the benzylic moiety and, hence, should remain nearly constant. This contention is supported by AM1 geometry optimizations on the anti conformer of 2′-Cl compound **3**: over a range in θ of 22–33°, H4–H6′ varied no more than ±0.02 Å from the value given in Table V and the associated enthalpy differences were essentially nil, again suggesting that these molecules are quite flexible. We have, therefore, adopted the *sp* uncertainties for the *ap* conformers. The geometrical parameters for the *ap* conformers are given in Table VI. The resulting fraction synperiplanar conformer (f_s) for each compound, as calculated from eq 3 and the error propagation analysis, as well as the *sp*/*ap* equilibrium ratio (K_{eq}) is given in Table I.

Though outside the restricted goals for the AM1 calculations in this work, we include here a summary of certain electronic details that may be of more general interest. The AM1 description of conjugation in a 1,4-dihydropyridine ring system may be gauged conveniently by calculated bond orders for the C=C and C—N bonds. In addition, the hybridization at N1 may be approached by considering the geometry about that atomic center.

AM1 geometry optimization of 2,6-dimethyl-1,4-dihydropyridine (considered as a model system) shows less ring puckering at C4 ($d_C = 0.077$ Å) than do the 4-aryldihydropyridines (Table IV), but a comparable amount of puckering at N1 ($d_N = 0.148$ Å). In the model system, the C=C and C—N bond orders are 1.81 and 1.03, respectively, and the N—H bond makes a dihedral angle of 140° with the C2–N1–C6 plane, indicating hybridization at N1 tending toward sp^3.

In the 2′-chloro analogue **3**, the bond orders were found to be rather insensitive to the syn/anti phenyl ring orientation, ranging between 1.68 and 1.72 for C=C and 1.06 and 1.08 for C—N. Note, however, that the C=C bonds are more delocalized through conjugation with the ester groups at C3/C5. The geometry at N1 depends upon the phenyl ring orientation, with the N–H bond dihedral angle (defined above) at 156° in the synperiplanar conformation and at 179° in the antiperiplanar conformation, so that the latter represents effectively pure sp^2 hybridization at N1.

Vasorelaxant Assay. Male New Zealand white rabbits (1.5–3 kg) were sacrificed by an overdose of sodium pentobarbital injected into the marginal ear vein. The thoracic aorta was quickly removed, rinsed of blood, and carefully cleaned of connective tissue in physiological salt solution (PSS) at room temperature. Circumferential strips of rabbit thoracic aorta were mounted for isometric force recording between two gold clips. The lower clip was connected to a calibrated micrometer for control of muscle length and the upper clip to a Grass FT.03 force transducer and a Grass Model 7D polygraph recorder. The mounted strips were placed in water-jacketed muscle chambers at 37 °C and aerated with 95% O_2 and 5% CO_2 (pH 7.4) in PSS containing (in mM) 111 NaCl, 5 KCl, 1 KH_2PO_4, 1.2 $MgSO_4$, 1.25 $CaCl_2$, 11.5 D-glucose, and 25 $NaHCO_3$.

During a 1–2-h equilibration period, the strips were slowly stretched to 4 g resting force. Test compounds were dissolved in 95% ethanol such that the final concentration of ethanol in the muscle bath was always less than 0.01%. Contractions were elicited by stimulation with 100 mM KCl (equimolar substitution for NaCl). When force reached a steady-state value, the solution was changed to one containing 100 mM KCl plus an appropriate concentration of test compound. The tissues were allowed sufficient time to relax to a new steady-state force. Each strip was exposed to only one concentration of one test compound, so that noncumulative concentration response curves could be obtained.

The levels of force maintained in the presence and absence of test compound were compared to calculate percent relaxation. IC_{50} values (concentration of test compound that caused 50% relaxation) and 95% confidence intervals were calculated from a logit transformation of the relaxation data obtained from at least four strips from individual rabbits for each of at least three concentrations of test compound. This test has been shown to be highly predictive of calcium channel blockade in those compounds in which IC_{50} values are less than 1 μM.[14]

Radioligand–Dihydropyridine Receptor Binding Assay. Male guinea pigs were sacrificed by placement in a saturated CO_2 atmosphere until respiration was inhibited. The hearts were excised and immediately placed in ice-cold Tris-isosaline (50 mM Tris in 0.154 M NaCl, pH 7.4) containing 0.1 mM EGTA. The tissues were finely minced with scissors and homogenized with a Polytron (Brinkman PT35, setting 7 for 15 s). The homogenates were centrifuged at 1000*g* for 20 min (4 °C). The resulting membrane pellet was washed four times in 10 mL of ice-cold Tris-isosaline (EGTA-free, containing 1 mM $CaCl_2$) per g of tissue wet weight. One hundred microliters of the ice-cold membrane solution (100–175 μg of protein) was added to 0.06–1.0 nM of 5-methyl[^{3}H]nitrendipine from New England Nuclear (NET741, 70–90 Ci/mmol) and appropriate concentrations of competing drugs in a final volume of 0.250 mL of Tris-isosaline containing 0.2% bovine serum albumin (BSA) and 2.5% ascorbic acid. The binding reaction was carried out in new disposable polypropylene tubes (Sarstedt #55.538) which were incubated in a water bath at 25 °C, starting immediately after administration of the membrane suspension. After the desired time of incubation (equilibrium established at 25 min of incubation), the samples were diluted 40-fold by addition of 10 mL of ice-cold Tris-isosaline and rapidly filtered under vacuum pressure through glass fiber filter disks (Schleicher and Schuell ZE 22, #30) with a Millipore Sampling Manifold apparatus. The filters were washed with 2 volumes of 5 mL of ice-cold Tris-isosaline, dried under vacuum pressure, and soaked in 10 mL of Aquasol scintillation fluid (New England Nuclear). Each sample was counted for 5 min in a Packard Tri-Carb 4640 scintillation counter. Specific binding of NTP was determined as the binding detectable in the absence ("total" binding) minus that in the presence of 2 μmol of unlabeled nifedipine ("nonspecific" binding). Specific binding routinely amounted to 75–85% of total binding. The amount of radioligand bound never exceeded 5% of the total amount of radioligand added in each assay.

The determination of the affinity of the radioligand for its specific binding site was made from a kinetic analysis of time-course studies of radioligand association and dissociation. The density of recognition sites in a tissue sample was determined by analysis of saturation binding data with a computer-aided nonlinear regression analysis of the unmodified binding data (cpm) or by linear regression analysis of the calculated saturation isotherm according to Scatchard.[40] Protein concentrations were

(40) Scatchard, G. *Ann. N.Y. Acad. Sci.* **1949**, *51*, 660.

determined according to the method of Bradford.[41]

For analysis of binding characteristics of nonlabeled test compounds, binding assays were performed with 32 concentrations of the competitive drug, each logarithmic decade subdivided into five increments and each concentration step assayed in duplicate. This protocol allowed for a total concentration range of more than six logarithmic decades to be covered in each separate concentration–effect curve (i.e., the highest concentration = 2×10^6 times the lowest concentration studied) and, thus, provided a high-resolution sequence of data points.

Graphic analysis of the data were performed by a computer-aided nonlinear regression, using a least-squares curve-fitting procedure. Assuming simple Michaelis–Menten kinetics of the interaction between radioligand and competing drug on any hypothesized number of coexpressed specific receptor types, the computation procedure fit the sigmoidal concentration effect curve defined by the law of mass action to the untransformed data. The analytical procedure allows for evaluation of the affinity of the competing drug for one or more subtypes of receptors that the radioligand nonselectively recognizes as specific binding sites. Calculation of K_d from the observed IC_{50} value (concentration of test compound that caused 50% inhibition of specific binding of NTP) was performed according to Cheng and Prusoff.[42] Multicomponent curve fitting furthermore allows for determination of relative density of receptor subtypes. It should be emphasized that accurate determination of specific/nonspecific binding ratio of the radioligand is absolutely essential for validation of multicomponent curve analysis.

All compounds were dissolved in 99% ethanol at a concentration of 1 mM and diluted 1000-fold in Tris-isosaline containing 0.2% BSA and 2.5% ascorbic acid. The final concentration of ethanol in the incubation cocktail was thus less than 0.02%, which has previously been found to be without detrimental effect on receptor integrity in the plasma membrane.[43] For a valid calculation of specific binding, the total binding assays (absence of nifedipine) contained the same concentration of ethanol as the nonspecific binding assays.

Acknowledgment. We thank Joseph Schwartz, Kaye Smillie, Russell J. Brittain, and Ophelia Hadjilambris for technical assistance, Mary Young and her associates for microanalytical data, and Alicia Kahle for nuclear magnetic resonance data.

Note Added in Proof

Subsequent to submission of this manuscript, there appeared a report of another ortho-substituted phenyl-1,4-dihydropyridine analogue that was observed to crystallize in the antiperiplanar conformation.[45]

Registry No. 1, 32947-20-9; 2, 21881-77-6; 3, 43067-01-2; 4, 112969-06-9; 5, 112969-07-0; 6, 21829-30-1; 7, 21829-09-4; 2-Cl-3-$NO_2C_6H_3CO_2H$, 3970-35-2; 2-Cl-3-$NO_2C_6H_3CH_2OH$, 89639-98-5; 2-Cl-3-$NO_2C_6H_3CHO$, 58755-57-0; $AcCH_2CO_2Me$, 105-45-3; 2-Cl-4-$NO_2C_6H_3CHO$, 5568-33-2; nifedipine, 21829-25-4.

Supplementary Material Available: Tables of atomic coordinates, thermal parameters, bond distances, and bond angles (33 pages). Ordering information is given on any current masthead page.

(41) Bradford, M. M. *Anal. Biochem.* **1976**, *72*, 248.
(42) Cheng, Y.-C.; Prusoff, W. H. *Biochem. Pharmacol.* **1973**, *22*, 3099.
(43) Bolger, G. T.; Gengo, P. J.; Luchowski, E. M.; Siegel, H.; Triggle, D. J.; Janis, R. A. *Biochem. Biophys. Res. Commun.* **1982**, *104*, 1604.
(44) Bossert, F.; Horstmann, H.; Meyer, H.; Vater, W. *Arzneim.-Forsch.* **1979**, *29*, 226; S. African Patent ZA 68/1482, 1968.
(45) Fossheim, R. *Acta Chem. Scand., Ser. B* **1987**, *B41*, 581.

Indoline Analogues of Idazoxan: Potent α_2-Antagonists and α_1-Agonists

Gay P. Fagan,* Christopher B. Chapleo, Anthony C. Lane, Malcolm Myers, Alan G. Roach, Colin F. C. Smith, Michael R. Stillings, and Anthony P. Welbourn

Departments of Medicinal Chemistry and Biology, Reckitt and Colman plc, Kingston-upon-Hull, HU8 7DS United Kingdom.
Received July 22, 1987

The synthesis and α-adrenergic activity of a series of substituted 2-imidazolinylindolines are described. Substitution in the indoline ring generated compounds with a spectrum of adrenoceptor antagonist/agonist profiles that proved sensitive to both the nature and position of the substituent. Many of the derivatives possess greater presynaptic antagonist potency than the corresponding benzodioxan 1, dihydrobenzofuran 2, and indan 3 analogues; however, this α_2-antagonism is often accompanied by α_1-agonist activity. It was not possible to separate α_2-antagonist from α_1-agonist properties in this series. Compounds of most interest proved to be the *N*-ethyl 6, 5-chloro-*N*-methyl 18, and 5-chloro-*N*-ethyl 23 derivatives, all being potent α_2-antagonists and α_1-agonists. Substitution at the 4- and 7-position of the indoline ring generally gave compounds with nonselective agonist properties.

The synthesis and pharmacological activities of a wide range of analogues of the potent and selective α_2-adrenoreceptor antagonist idazoxan (1) have been reported[1-3] in which the effects of substitution and modification of the dioxan and imidazoline rings were examined. The replacement of the dioxan ring in 1 by a variety of six- and five-membered heterocyclic systems has in many cases proven deleterious in terms of α_2-antagonist potency and selectivity.[2] From our own investigations the dihydrobenzofuranylimidazoline 2 has emerged as the only analogue possessing prejunctional antagonist potency and selectivity comparable to that of 1, although the corresponding indanylimidazoline 3 has also been described as a potent α_2-antagonist by other workers.[4]

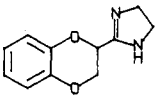

1

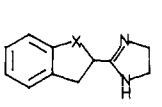

2 X = O
3 X = CH_2

(1) Part 1: Chapleo, C. B.; Myers, P. L.; Butler, R. C. M.; Doxey, J. C.; Roach, A. G.; Smith, C. F. C. *J. Med. Chem.* **1983**, *26*, 823.
(2) Part 2: Chapleo, C. B.; Myers, P. L.; Butler, R. C. M.; Davis, J. A.; Doxey, J. C.; Higgins, S. D.; Myers, M.; Roach, A. G.; Smith, C. F. C.; Stillings, M. R.; Welbourn, A. P. *J. Med. Chem.* **1984**, *27*, 570.
(3) Part 3: Stillings, M. R.; Chapleo, C. B.; Butler, R. C. M.; Davis, J. A.; England, C. D.; Myers, M.; Tweddle, N.; Welbourn, A. P.; Doxey, J. C.; Smith, C. F. C. *J. Med. Chem.* **1985**, *28*, 1054.
(4) Bigg, D.; Menin, J. FR 2542738A; *Chem. Abstr.* **1986**, *105*, 129906*v*.

0022-2623/88/1831-0944$01.50/0